NASA Technical Memorandum 87645

SUPERSONIC AERODYNAMIC CHARACTERISTICS OF SOME REENTRY CONCEPTS FOR ANGLES OF ATTACK TO 90°

M. LEROY SPEARMAN

NOVEMBER 1985

NASA
National Aeronautics and Space Administration

Langley Research Center
Hampton, Virginia 23665

SUMMARY

Past studies of reentry vehicles tested to high angles of attack (up to 90°) in the Mach number range from 2 to 4.8 have been examined with a view toward the potential usefulness of such concepts in a flight regime that would include reentry from space into the atmosphere followed by a transition to sustained atmospheric flight. Two basic planforms were considered--highly-swept deltas and circular. The delta concepts included variations in cross section (and thus volume) and in camber distribution. The effectiveness of various types of aerodynamic control devices was also included.

Both the highly-swept delta and the circular planforms were found to be possible candidates for transitional flight since stability and control could be maintained over the angle-of-attack range.

INTRODUCTION

Early studies of spacecraft included concepts that would reenter the atmosphere at very high angles of attack in order to produce drag for deceleration. Following the deceleration, such vehicles would then perform a transition to lower angles of attack to provide for sustained atmospheric flight with extended range and maneuver capability. This kind of transitional flight would be required for the development of transatmoshperic vehicles which was one of the three goals outlined in April of this year by the Aeronautical Policy Review Committee of the White House Office of Science and Technology Policy.

The purpose of the present paper is to review the aerodynamic behavior of some previously conceived reentry concepts for angles of attack up to 90°. Such a review will provide useful insights into the stability and control characteristics, lift and drag characteristics, and some effects of planform and volume variations, which, in turn, will indicate some of the trades to be considered in developing a vehicle for transatmospheric operation.

SYMBOLS

C_D	drag coefficient
C_L	lift coefficient
C_m	pitching-moment coefficient
C_{l_β}	effective dihedral parameter
C_{n_β}	directional stability parameter
L/D	lift-drag ratio
L.E.	leading edge

M	Mach number
c	chord length
ι	body length
t	thickness
c.g.	center of gravity
α	angle of attack, deg.
δ	control deflection, deg.
Λ	sweep angle, deg.

Coefficients for the configurations presented herein are nondimensionalized in various ways. Detailed information for the configurations may be found in the referenced papers. The numerical value of the coefficients, however, does not affect the interpretation of the results.

DISCUSSION

CROSS-SECTION CONCEPTS

One of the early studies of high-angle-of-attack high-drag reentry vehicles (ref. 1) contains M=2 results for two series of blunted delta planform concepts with several cross-sectional shapes for angles of attack from 0° to 90°. Some of these concepts, shown in figures 1 and 2, consisted of blunted delta planforms of 75° and 80° leading-edge sweep angles. The cross-sections were circular, cruciform elliptical, horizontal elliptical, and a flat-plate wing with a top-mounted body. The models had equal planform areas and, thus, substantial variations in volume. Controls consisting of retractable canards and aft-split flaps were investigated on the 80° cruciform elliptical model (fig. 2).

The effect of cross-section on the pitching moment variation with angle of attack for the 75° sweep configurations is shown in figure 3. For a constant c.g. location of 0.61 body length, the pitching moments vary from a highly stable trend for the circular cross section to a progressively less stable trend as the configuration is flattened. This trend probably results from a combination of increased retention of forebody lift on the lower surface and increased flow separation over the upper afterbody as the lifting surface is flattened. Of the four configurations, configuration II (cruciform ellipse) appears to be the most linear over the angle-of-attack range although each display a reflex between angles of attack of about 40° to 60°. The flat wing-body concept resulted in an undesirable negative pitching moment at zero angle of attack because of the forebody shape and the interference flow induced by the forebody on the wing upper surface apex lift.

Pertinent lift and drag characteristics for the various 75° concepts are shown in bar-graph form in figure 4. The characteristics shown are the drag at zero angle of attack, drag at 90° angle of attack, maximum lift, and maximum lift-drag ratio. The flat wing-body configuration (IV) indicates the lowest drag at zero angle of attack, the highest drag at 90° angle of attack, and the highest values of maximum lift and maximum lift-drag ratio--all of which are desirable traits. However, this configuration also has a negative value of pitching moment at zero angle of attack and a highly nonlinear variation of pitching moment with angle of attack--both of which are undesirable. Hence, trim control could become a critical factor for the flat-wing body.

The conical body (I) had the highest drag at zero angle of attack, the lowest drag at 90° angle of attack, and the lowest values of maximum lift and maximum lift-drag ratio. The elliptical body and the cruciform elliptical body display progressive variations between the extremes of IV and I. Hence, trades can be made between such things as volume requirements, pitching-moment linearity (trim), and lift and drag characteristics.

The effects of leading-edge sweep on the pitching-moment characteristics for configurations II and IV are shown in figure 5. For these data, the c.g. location has been adjusted to provide equal C_m (-0.08) at $\alpha = 90^0$. Increasing the sweep from 75° to 80° reduces the negative pitching-moment increment at zero angle of attack for configuration IV since there is less exposed wing surface to be affected by the body flow field. In addition, the pitching moment linearity is improved for both configurations II and IV since there is less exposed wing surface aft.

The lift and drag characteristics for the 80° sweep versions of configurations II and IV are compared in figure 6. As would be expected, the flat wing-body configuration (IV) provides higher values of lift and lift-drag ratio over the entire angle-of-attack range even though the drag is higher above an angle of attack of about 70°. Thus, while configuration IV displays some aerodynamic advantages for reentry flight at high angles and for sustained atmospheric flight at lower angles, it does so at the expense of decreased volume and with possible longitudinal trim penalties due to the negative pitching moment at zero angle of attack.

Some effects of longitudinal control devices are shown in figure 7 for the 80° sweep version of the cruciform ellipse configuration II. The control devices are shown in figure 2. The extension of a pivoting canard surface is quite effective in providing longitudinal trim over essentially the entire angle-of-attack range. The canard, of course, provides no control at zero angle of attack but a split-flap arrangement at the rear of the upper vertical ellipse was effective in providing trim up to about 25° angle of attack. Thus, through the combined use of an aft-split flap and a pivoting canard, it appears that longitudinal control could be provided over the entire angle-of-attack range.

Modified Delta-Wing Concept

Another flat delta-wing-body concept, extracted from reference 2, is shown in figure 8. The concept has a basic 73° delta wing, foldable cranked-wing-tip panels, a trailing-edge flap control, and a leading-edge flap control.

The longitudinal characteristics at M=2, including the effect of tip deflection, is presented in figure 9. The basic trends are similar to those for the previously discussed flat-wing-body concept (figs. 3 and 5) in that the negative increment of pitching moment at zero angle of attack and the nonlinearity characteristics are apparent. Varying the tip deflection from 0° to 90° results in significant reductions in longitudinal stability as would be expected although the regions of nonlinearity remain essentially the same. The lift and drag characteristics for the extreme tip deflections of 0° to 90° show effects that might be anticipated although the differences are relatively small (fig. 10).

Some longitudinal control characteristics with the tips deflected 90° are shown in figure 11. The addition of a trailing-edge flap provides increased longitudinal stability over the entire angle-of-attack range to 90° and a 60° deflection of the flap provides trim control to an angle of attack of about 30°. The extension of a leading-edge control (canard) begins to provide a positive control increment above an angle of attack of about 15°. Thus, through a combination of a trailing-edge flap and a leading-edge control, it appears that longitudinal trim and control could be provided over the entire angle of attack range.

75° Triangular Planform Concepts

Another series of triangular planform concepts with variations in cross section have been extracted from reference 3 and are shown in figure 12. These concepts have a basic sharp 75° triangular planform and include a cone, an ellipse, a modified ellipse with the upper surface contoured to represent a distinct body, and a flat-plate wing with a slender upper-surface body. These concepts were tested at angles of attack up to 90° at M=2.94, 3.87, and 4.78 (ref. 3).

Some longitudinal characteristics for the four concepts are shown in figure 13 for M=2.9. These characteristics are somewhat similar to those for the cross-section concepts previously discussed, that is:

- The maximum lift and lift-drag ratio were achieved with the flat-wing body
- The lowest lift and lift-drag ratio occurred with the conical body
- The drag at zero angle of attack was least with the flat-wing body and the greatest with the conical body

- The drag at 90° angle of attack was greatest with the flat-wing body and least with the conical body

All the configurations were longitudinally stable with the c.g. at 0.60 body length but a nonlinear variation was evident near an angle of attack of 50°. The modified ellipse indicates a unique characteristic in that, at zero angle of attack, lift is produced and a lift-drag ratio of four was obtained.

The longitudinal control characteristics for the flat-plate-wing body with plain trailing-edge flaps are shown in figure 14 for M=2.9. Use of the trailing-edge flap alone is insufficient to provide the trim or control required over the angle-of-attack range with the c.g. at 0.60 body length. As indicated on the figure, a shift of the c.g. to 0.54 body length would permit trim to 90° angle of attack. Of course, the additional use of forward controls would also relieve the trim limitations as illustrated with two of the previously discussed concepts (figs. 7 and 11).

Cambered Body Concepts

A series of cambered bodies having a basic blunted 75° triangular planform are shown in figure 15. These bodies, having variations in thickness ratio and in maximum thickness location, have been tested at angles of attack up to 53° for Mach numbers from 2.3 to 4.6 (unpublished).

The longitudinal characteristics at M=4.6 are presented in figure 16 for bodies with a flat top and variations in the lower surface camber. The body with a thickness ratio of 0.1 at 0.3c resulted in the lowest drag at the lower angles of attack and the highest lift-curve slope and, accordingly, has the highest maximum lift-drag ratio (about 2). However, for the test c.g. location of 0.53 body length, this configuration also had the lowest self-trimming potential (16°). Increasing the thickness ratio to 0.2 at either 0.3c or 0.5c resulted in increased drag over the lower angle-of-attack range and a reduction in lift-curve slope so that the maximum lift-drag ratio was reduced to about one. However, the potential for self trimming for these two configurations increased to 36° and 48°. Thus, for this illustration, the increased thickness and changes in thickness location result in bodies with greater volume and potentially better trim characteristics but at the expense of lower lift capability and lower maximum lift-drag ratios.

Further modifications to the body camber were examined in an effort to extend the self-trimming potential. One configuration incorporated an upper surface camber of 0.1 thickness ratio at 0.3c and a lower surface camber of 0.2 thickness ratio at 0.7c. This configuration is compared in figure 17 with the flat-top body having a lower-surface, camber-thickness ratio of 0.1 at 0.5c. This modification resulted in a substantial improvement in pitching-moment linearity with a potential self-trim point in excess of 53°. In addition, there is a further increase in a volume with essentially no change in lift characteristics and a small reduction in lift-drag ratio. It should be remembered that these results are for a body alone with no additional lifting

or control surfaces. It would be expected that the judicious use of other surfaces would provide further improvement.

The lateral-directional characteristics for the cambered-body concepts are presented in figure 18. The flat-top configurations with lower-surface camber variations are shown on the left. The configuration with the better lift-drag (t/c=0.1, 0.3c) and the configuration with the better trim potential (t/c=0.2, 0.5c) display lower levels of directional instability, particularly at the higher angles of attack. In addition, both exhibit a positive dihedral effect. Further modifications to both the upper-surface and lower-surface camber are compared on the right with the configuration having a flat top and the t/c=0.2, 0.5c lower-surface camber. Both configurations exhibit reasonably good directional characteristics. The addition of camber to the upper surface did result in a negative dihedral effect, however, presumably because of the added side area above the roll axis. Again, the addition of other surfaces would affect the lateral-directional characteristics.

Lenticular Body Concept

A lenticular concept (fig. 19) has been investigated to 90° at M=2 and to 56° at M=3.5 and 4.65 (ref. 5).

The longitudinal characteristics at M=2 are shown in figure 20. The addition of the fins results in increased lift as well as increased drag but with a small net increase in maximum lift-drag ratio. The fins considerably increase the longitudinal stability and because of the fin location, there is a positive increment in pitching moment at zero angle of attack that leads to a self-trimming point at about 15° for the test c.g. location of 0.45 body length.

The effects of longitudinal control deflection at M=2 (fig. 21) indicates that, for the test c.g., a -30° deflection provides trim at about 42° angle of attack. By shifting the c.g. forward, trim occurs at 62° for a c.g. at 0.40 body length and at 78° for a c.g. at 0.36 body length. The longitudinal control at M=3.5 (fig. 22) indicates trim in excess of 56° is readily attainable and that a self-trimming point (zero deflection) occurs at 32° with the c.g. at 0.45 body length.

The lateral-directional stability characteristics for the lenticular body to an angle of attack of 56° at M=3.5 are presented in figure 23. The results indicated directional stability up to 56° with the fins off. Adding the fins increased the directional stability up to about 46° above which the configuration was less stable with the fins on than with the fins off--probably because of an adverse sidewash in the vicinity of the fins. Such an effect does not occur at M=4.65 and the configuration (ref. 5), either fin on or off, is directionally stable to 56°. The configuration also provides a positive dihedral effect over the angle-of-attack range.

CONCLUDING REMARKS

It has been the purpose of this paper to present the aerodynamic characteristics of some reentry-type vehicles for an angle-of-attack range up to 90° in order to determine factors that might influence the design of concepts required to enter the atmosphere from space and perform a transition to sustained atmospheric flight.

Some concluding observations are:

- Highly-swept triangular planform configurations and a circular planform configuration were both found to be possible candidates for transitional flight.
- Control over the angle-of-attack range could be maintained with the triangular configurations with the best results being through the combined use of aft and forward controls.
- The thinner wing-body concepts tended to have the best aerodynamic efficiency but the least volume.
- Conversely, those arrangements having the greatest volume, although quite manageable, tended to have the least aerodynamic efficiency.
- The circular planform lenticular body, in addition to having good longitudinal trim characteristics, indicated good directional stability largely due to inherent stability of the body.

REFERENCES

1. Jackson, Charlie M., Jr.; and Harris, Roy V., Jr.: Investigation of Mach Number of 1.99 of Two Series of Blunted Delta Planform Models with Several Cross-Sectional Shapes for Angles of Attack from 0° to 90°. NASA TM X-543, 1961.

2. Foster, Gerald V.: Exploratory Investigation at Mach Number of 2.01 of the Longitudinal Stability and Control Characteristics of a Winged Reentry Configuration. NASA TM X-178, 1959.

3. Wiggins, Lyle E.; and Kaattari, George E.: Supersonic Aerodynamic Characteristics of Triangular Plan-Form Models at Angles of Attack to 90°. NASA TM X-568, 1961.

4. Jackson, Charlie M., Jr.; and Harris, Roy V., Jr.: Static Longitudinal Stability and Control Characteristics at a Mach Number of 1.99 of a Lenticular-Shaped Reentry Vehicle. NASA TN D-514, 1960.

5. McShera, John T., Jr.; and Lowery, Jerry L.: Static Stability and Longitudinal Control Characteristics of a Lenticular-Shaped Reentry Vehicle. NASA TM X-763, 1963.

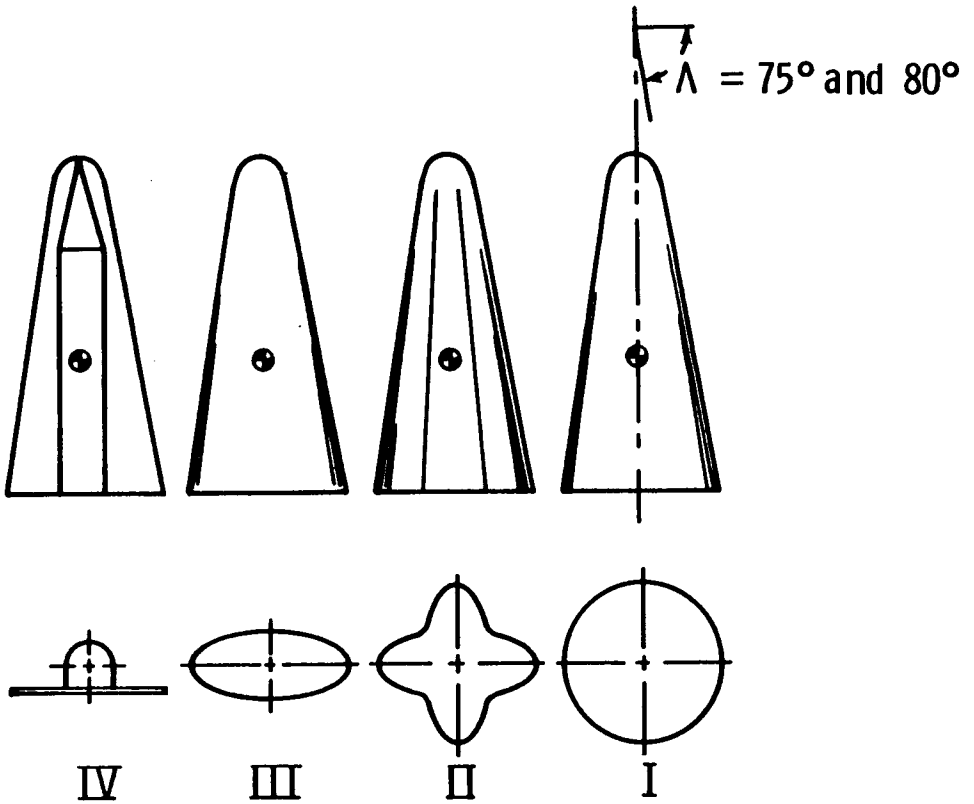

Figure 1.- Cross-section conceptual models.

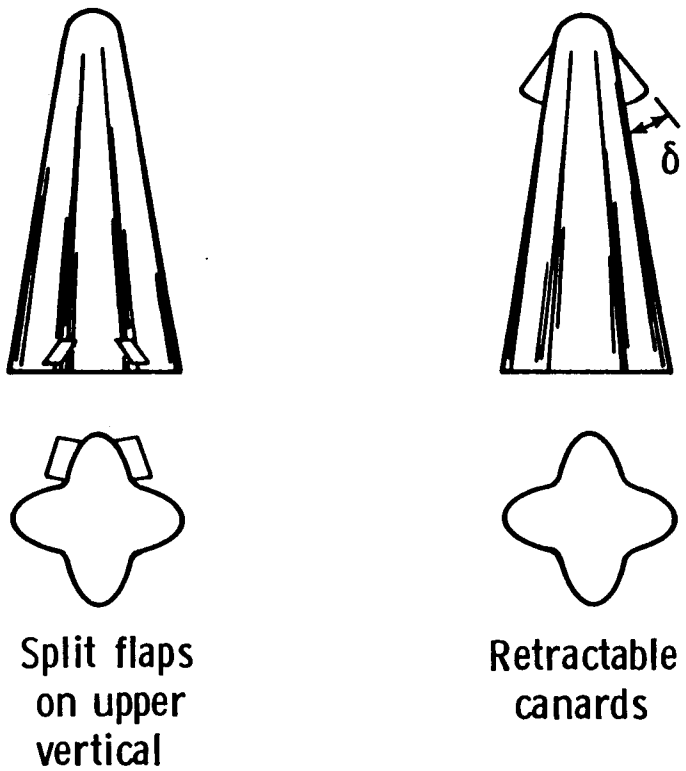

Figure 2.- Controls for cross-section model II, $\Lambda = 80^0$.

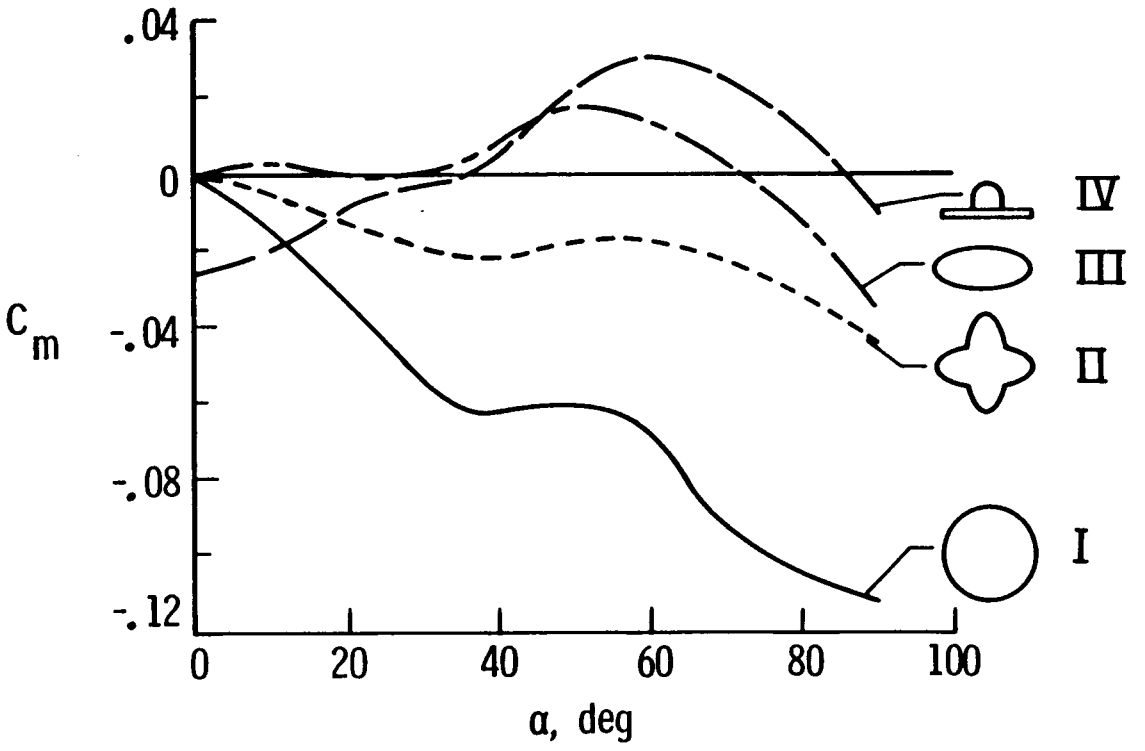

Figure 3.- Effect of cross-section on pitching moment, M = 2, $\Lambda = 75^0$, c.g. = 0.61 ℓ.

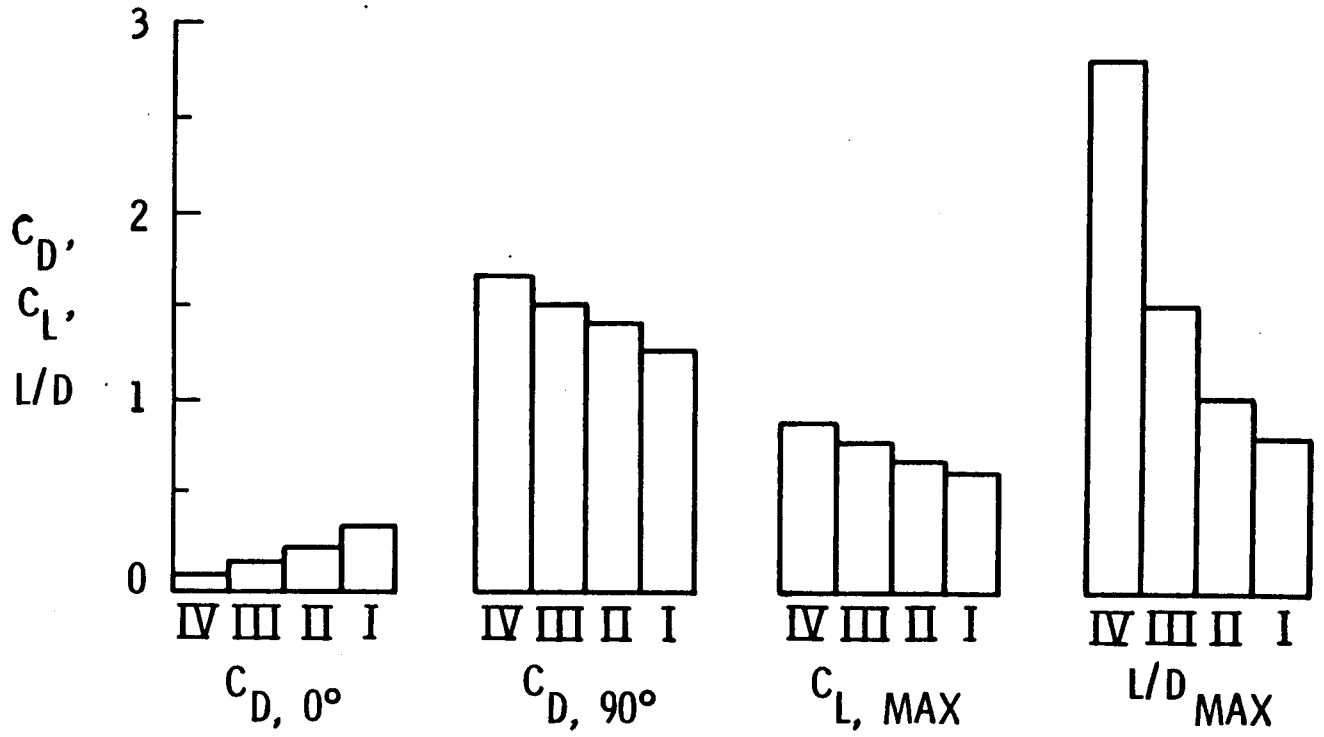

Figure 4.- Lift and drag summary for various cross sections, M = 2, $\Lambda = 75^0$.

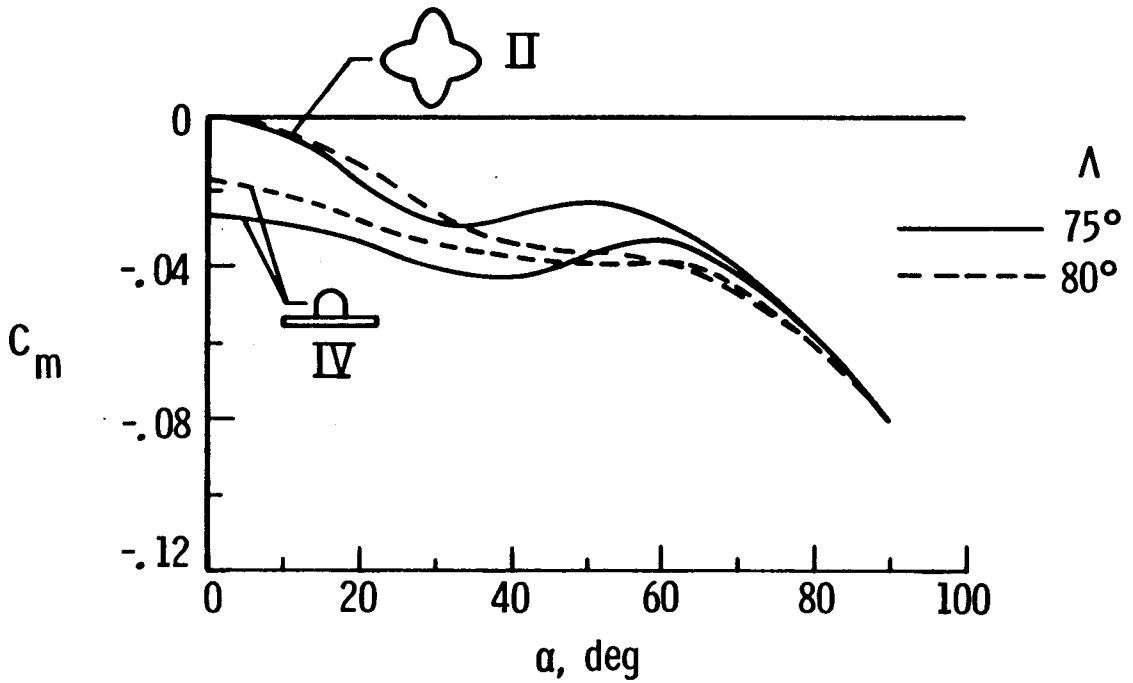

Figure 5.- Effect of sweep on pitching-moment for cross-section models II and IV, M = 2, c.g. adjusted to provide equal C_m at $\alpha = 90^0$.

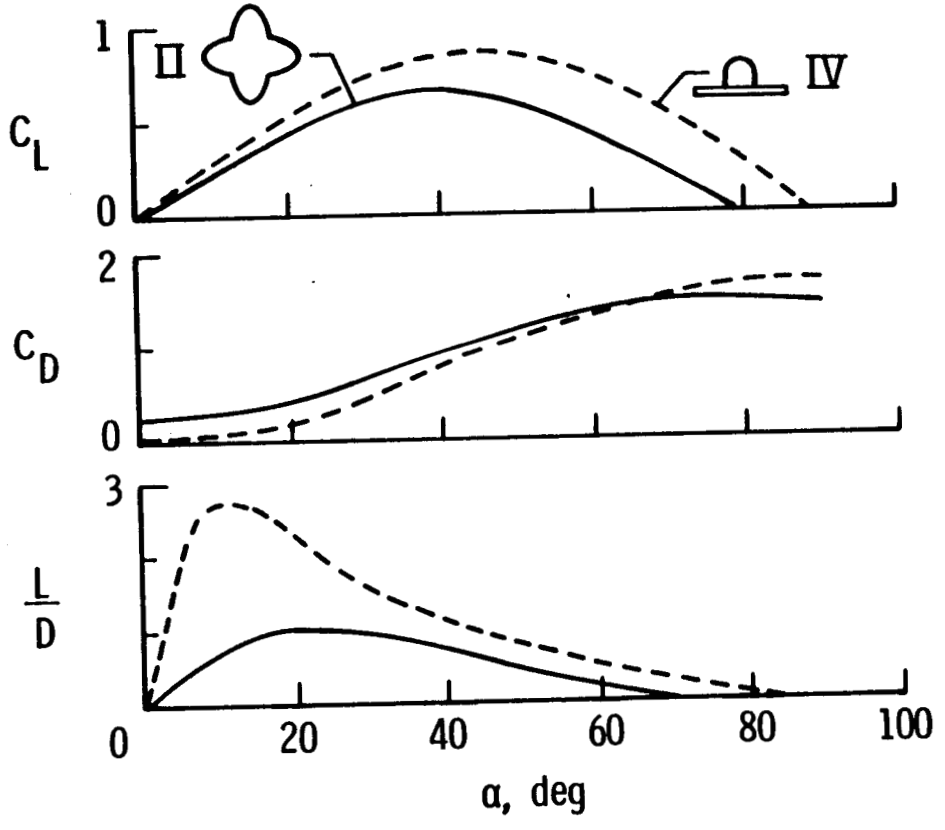

Figure 6.- Lift and drag characteristics for cross-section models II and IV, M = 2, $\Lambda = 80^0$.

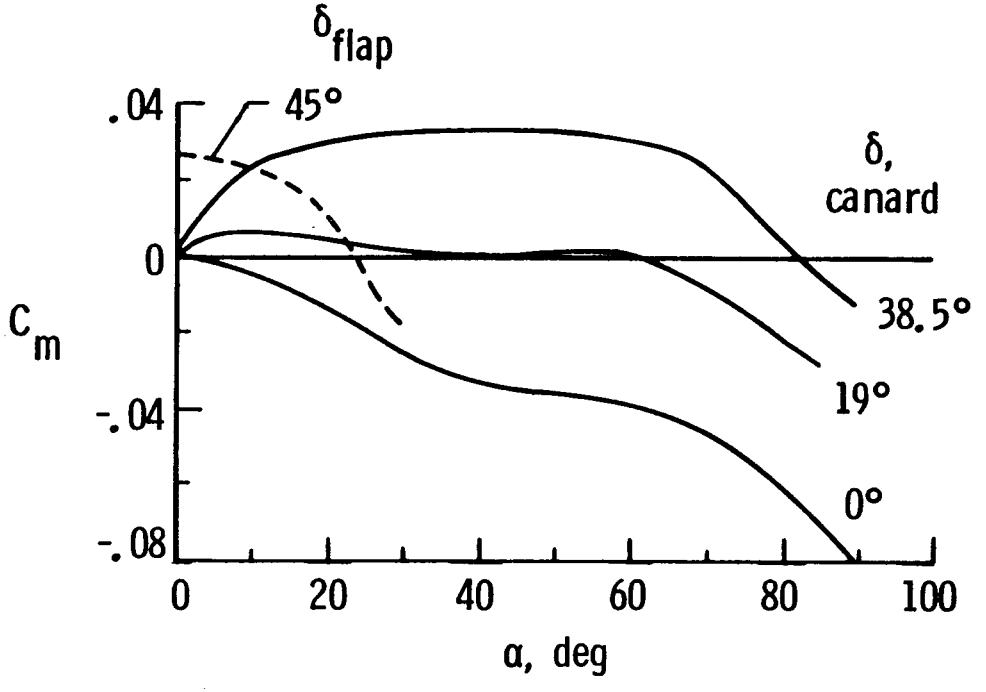

Figure 7.- Longitudinal control for model II, M = 2, $\Lambda = 80^0$, c. g. = 0.61 ℓ.

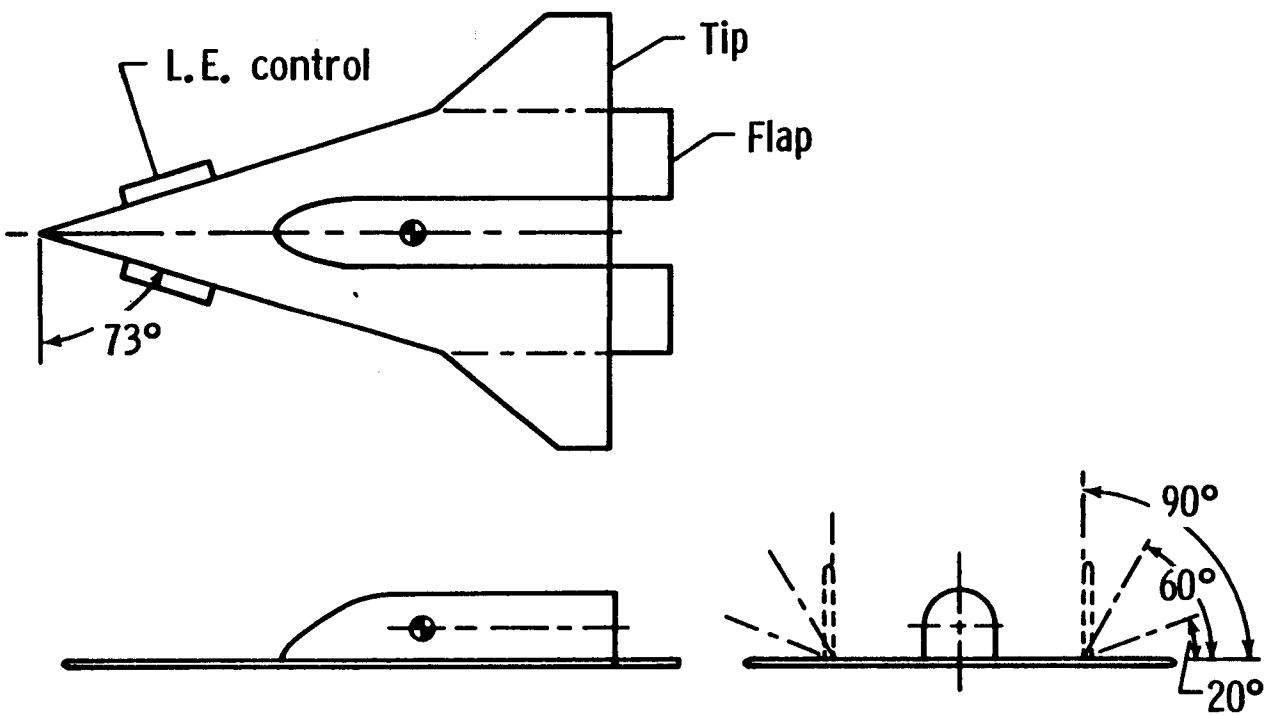

Figure 8.- Modified delta wing model.

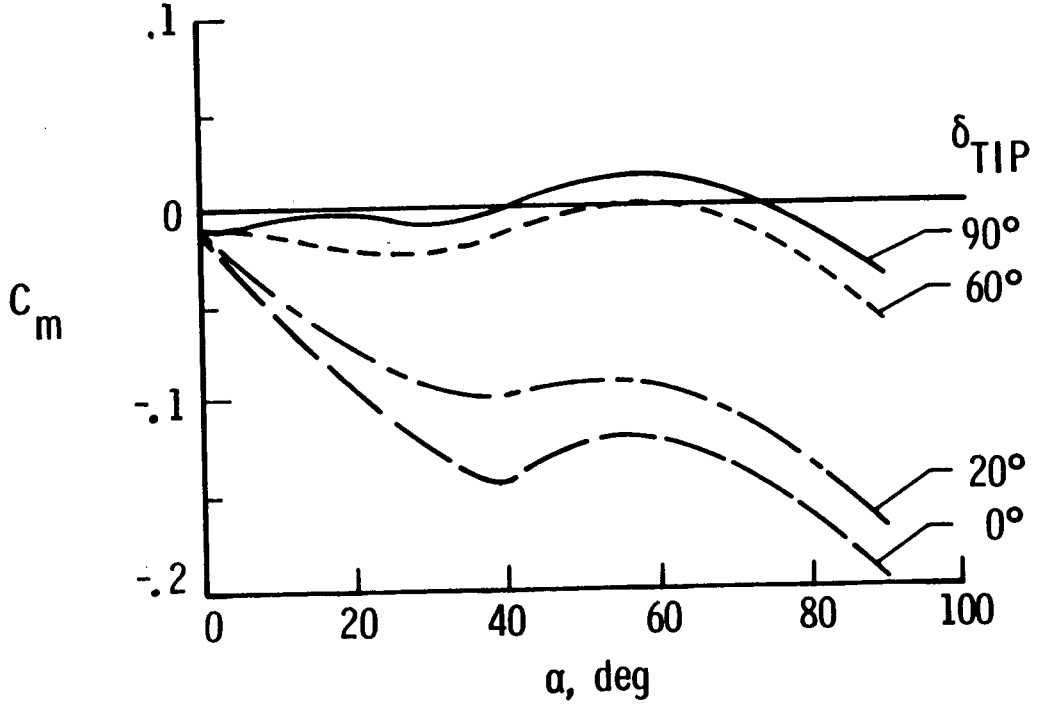

Figure 9.- Effect of tip deflection on pitching moment, modified delta wing model, M = 2, c.g. = 0.64 ℓ.

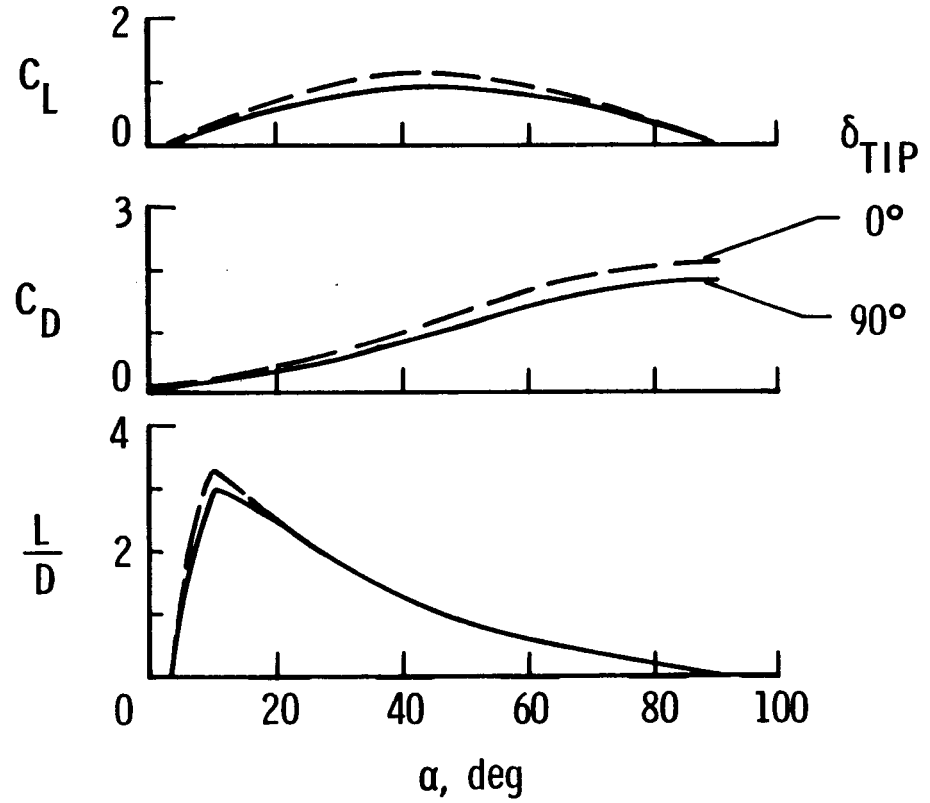

Figure 10.- Lift drag characteristics, modified delta wing model, M = 2.

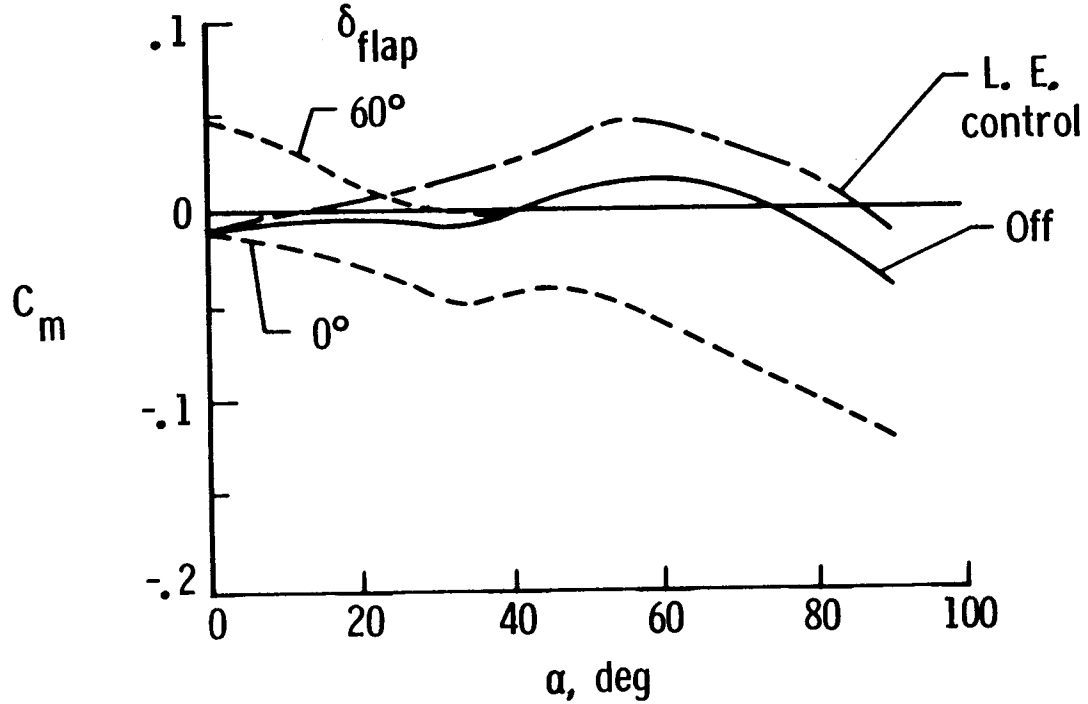

Figure 11.- Longitudinal control, modified delta wing model, M = 2, $\delta_{tip} = 90^0$, c. g. = 0.64 ℓ.

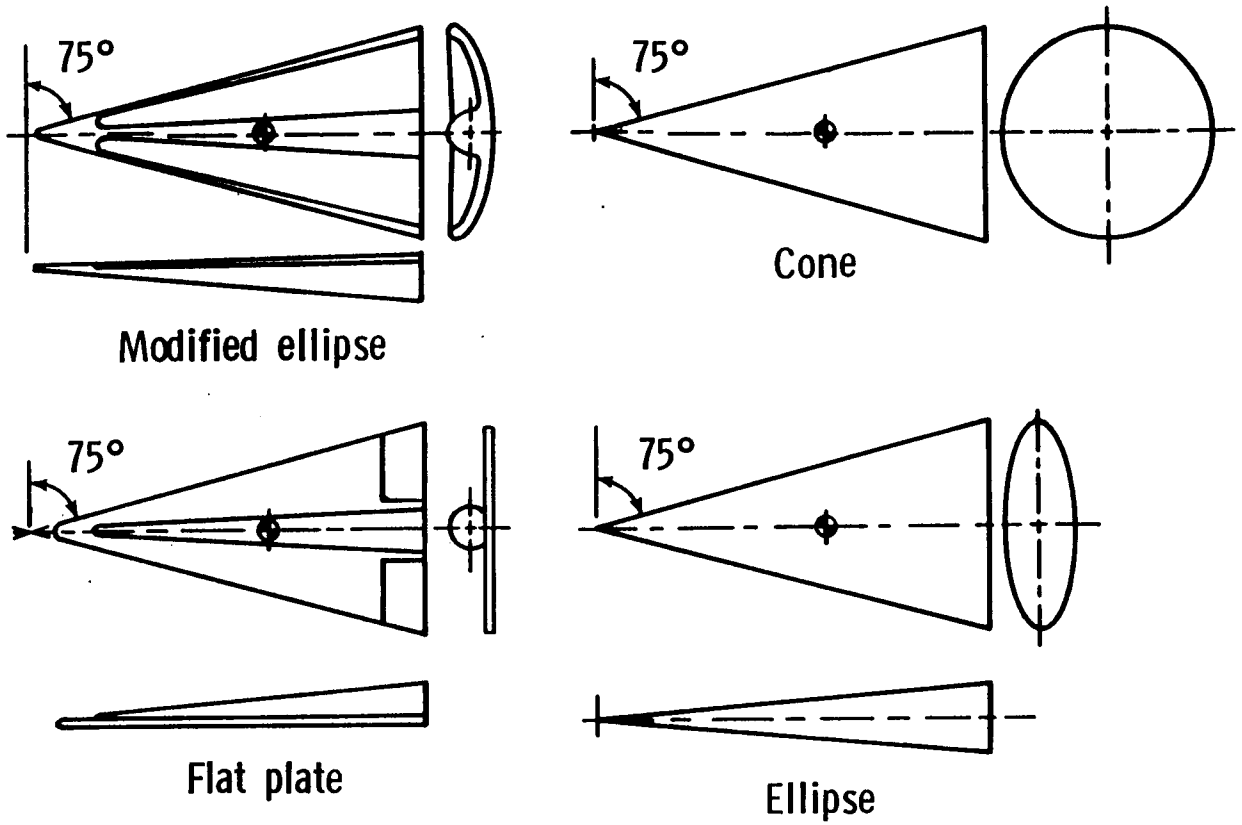

Figure 12.- 75° triangular planform models.

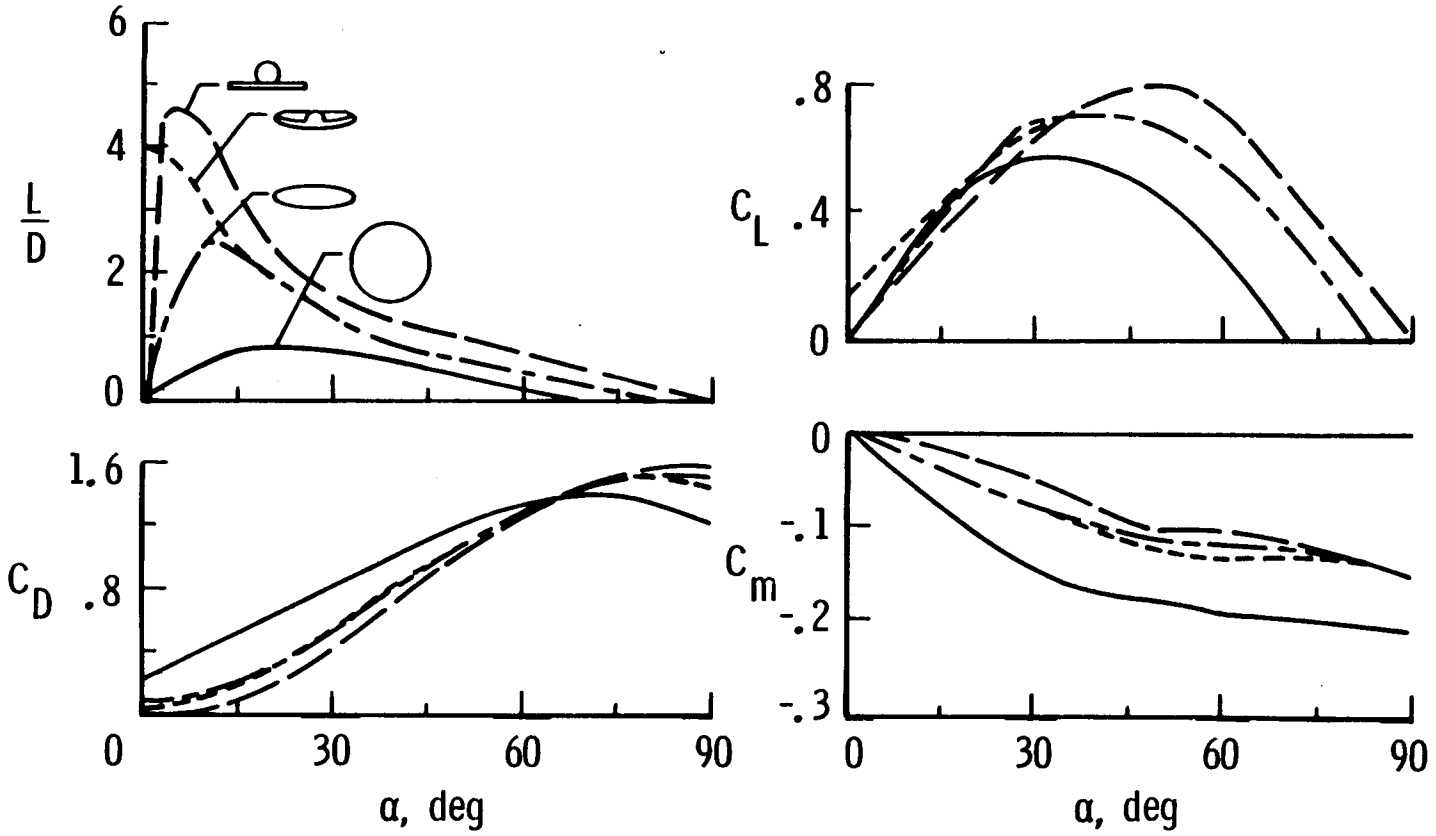

Figure 13.- Longitudinal characteristics, 75° triangular planform models, M = 2.9, c. g. = 0.60 ℓ.

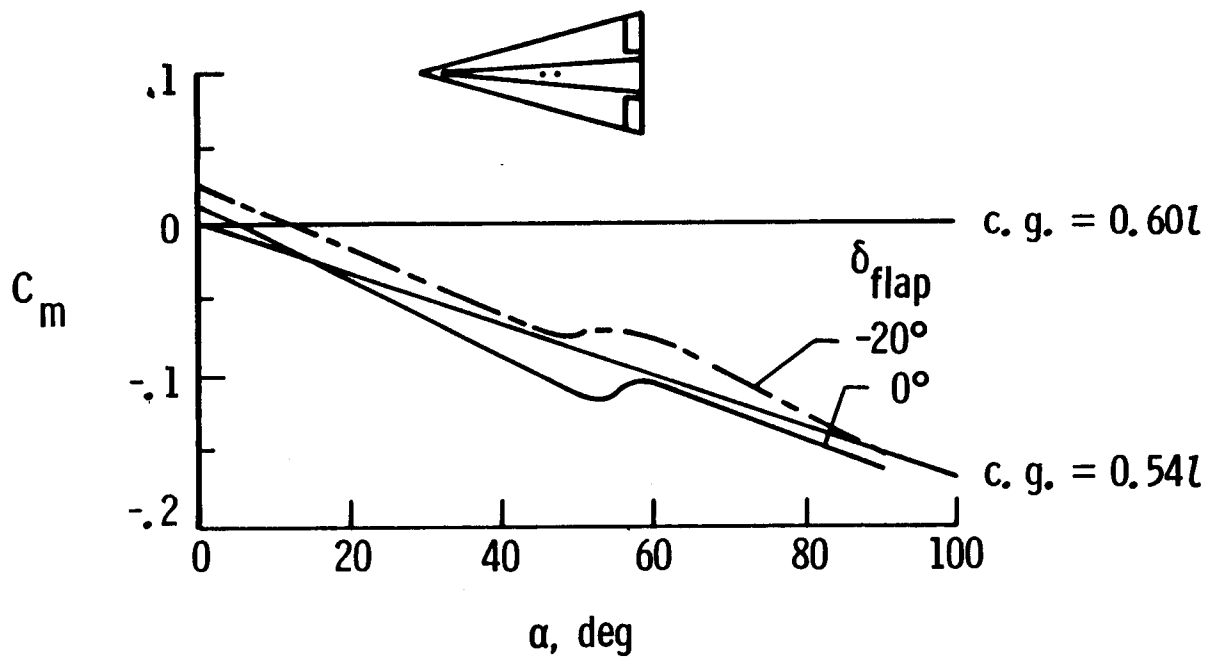

Figure 14.- Longitudinal control, flat plate 75° triangular planform model. M = 2.9.

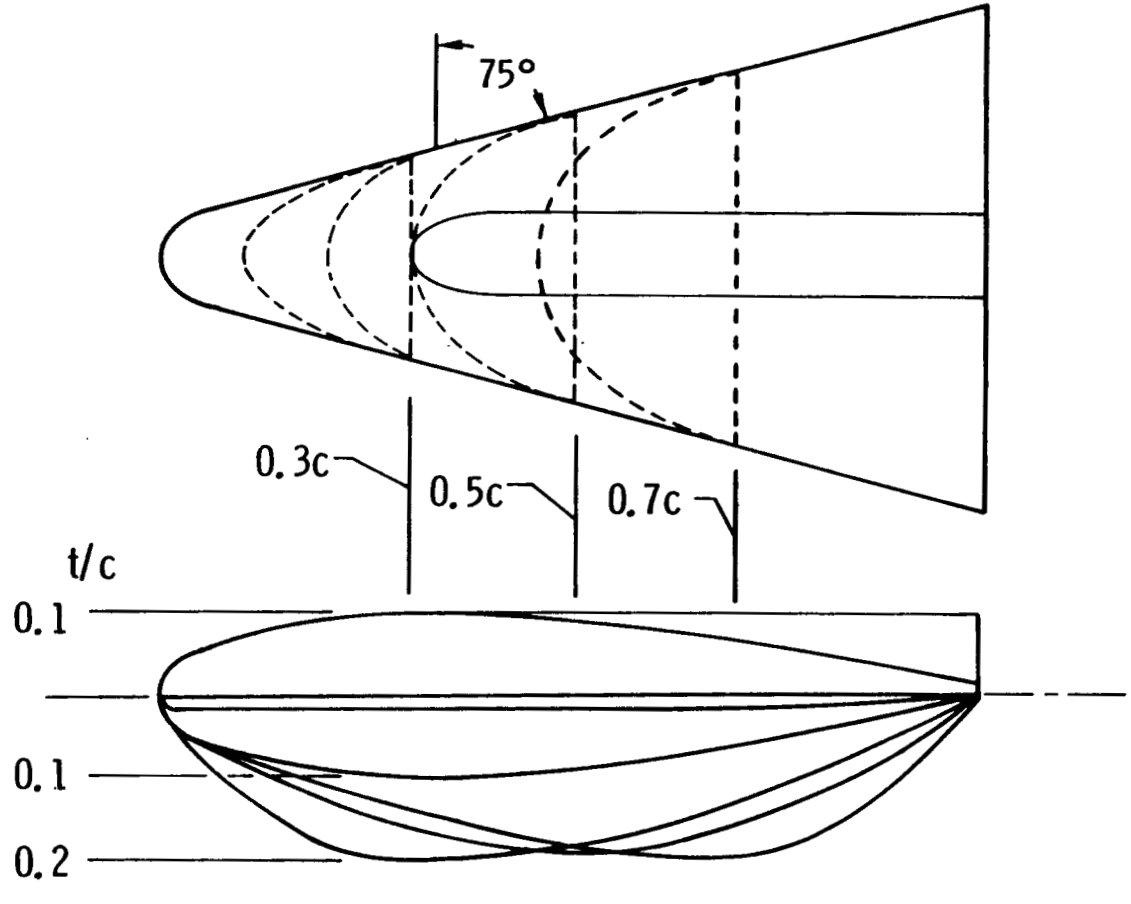

Figure 15.- Cambered bodies with 75° triangular planform.

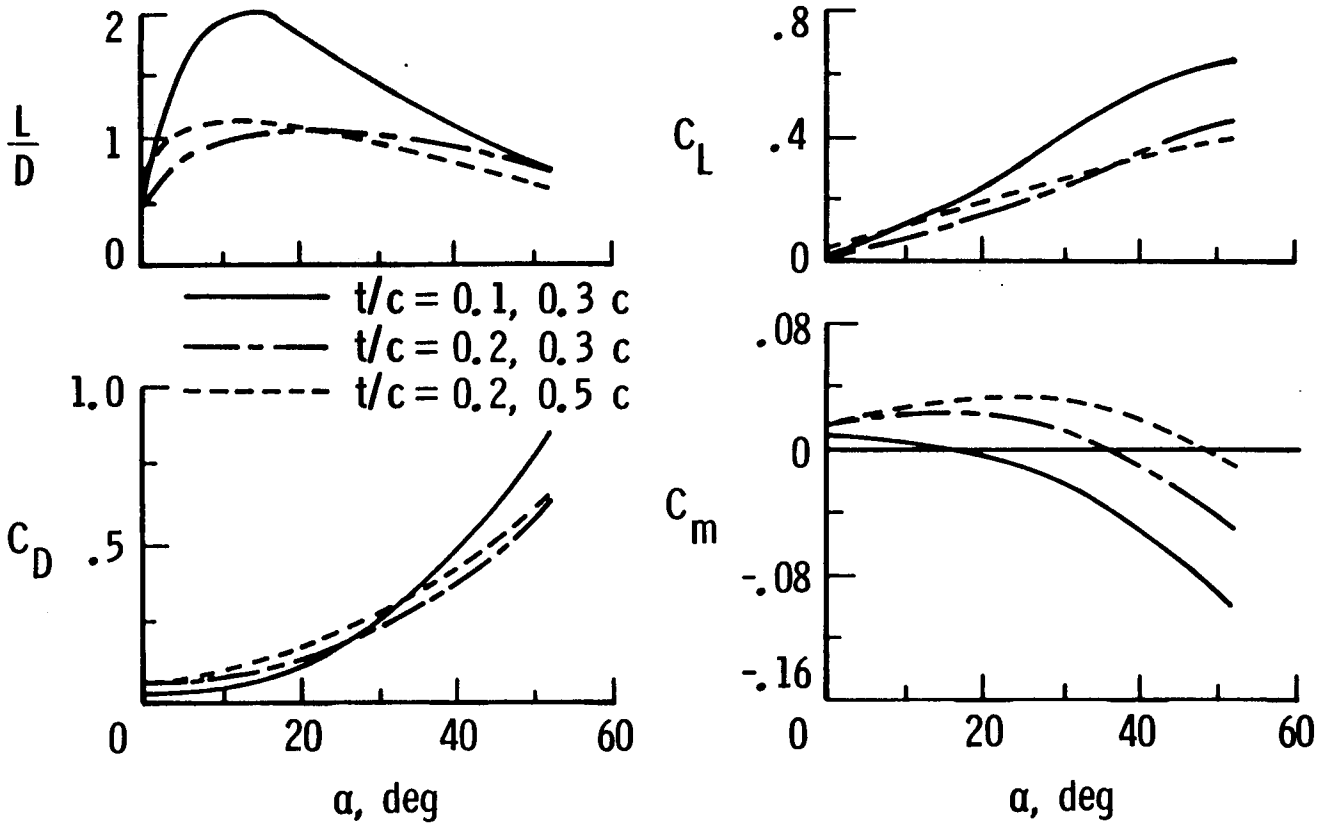

Figure 16.- Effect of lower surface camber with flat top, 75° triangular planform, M = 4.6, c.g. = 0.53 ℓ.

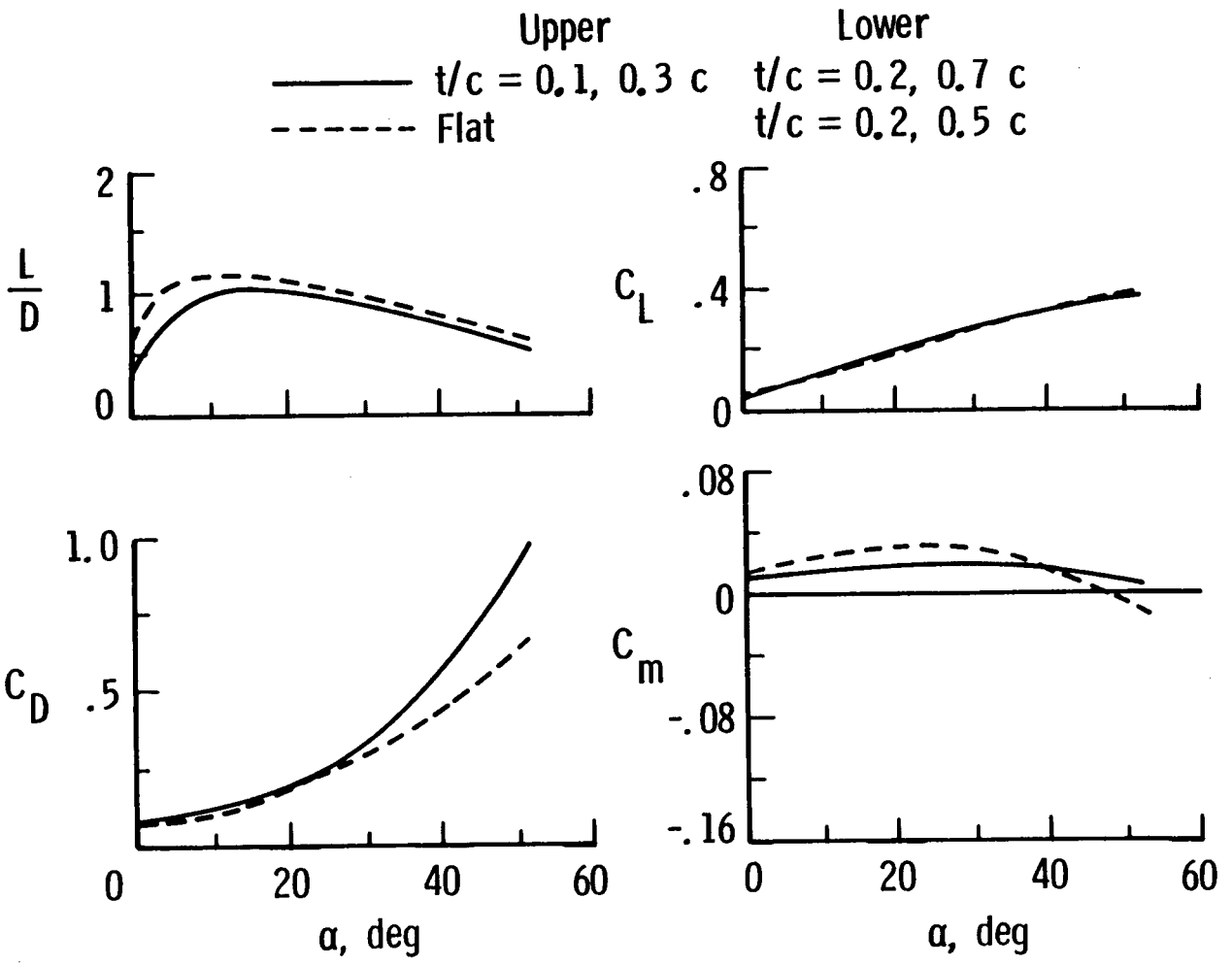

Figure 17.- Some effects of upper and lower surface camber, 75° triangular planform, M = 4.6, c. g. = 0.53 ℓ.

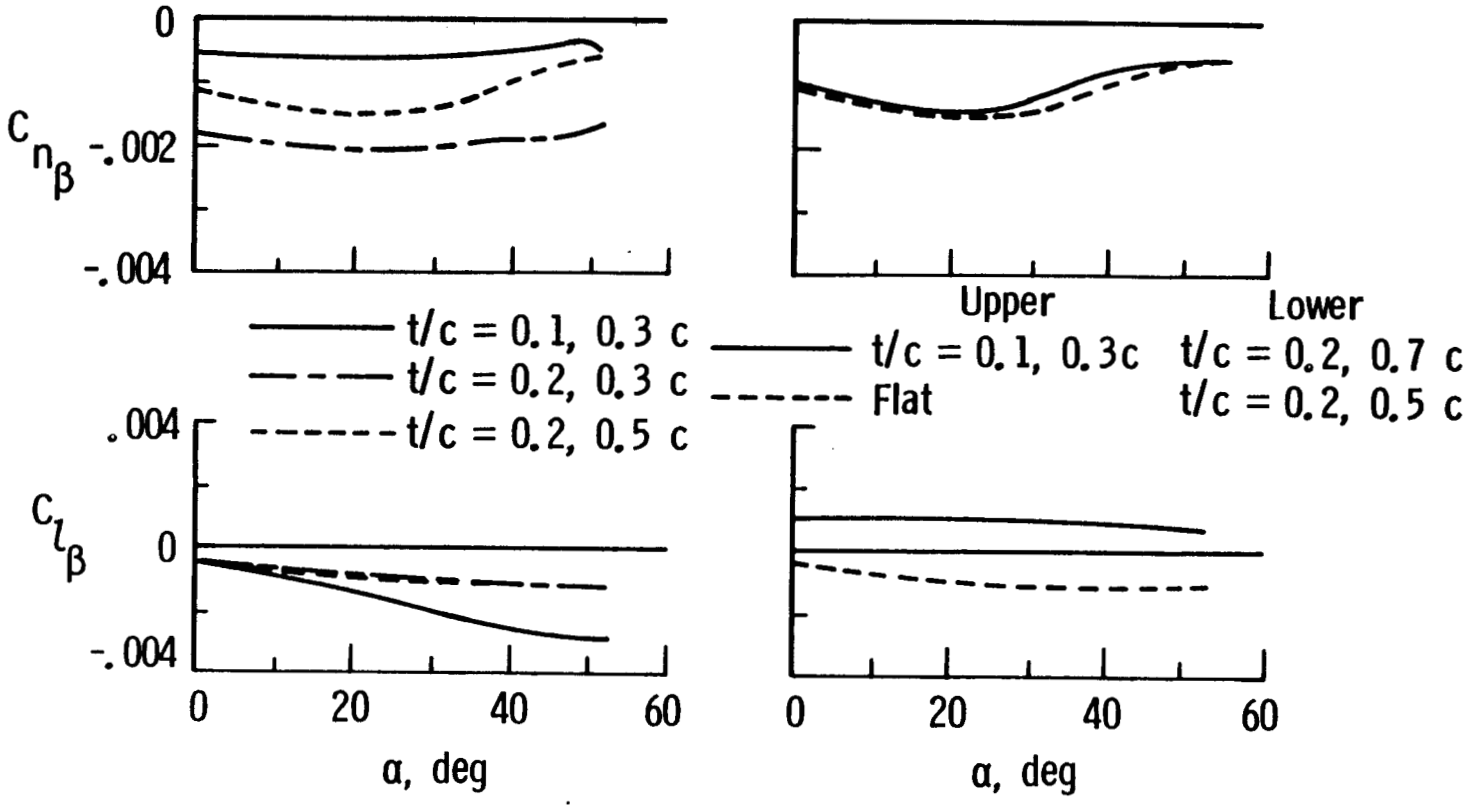

Figure 18.- Lateral-directional characteristics, 75° triangular planform, M = 4.6, c.g. = 0.53 ℓ.

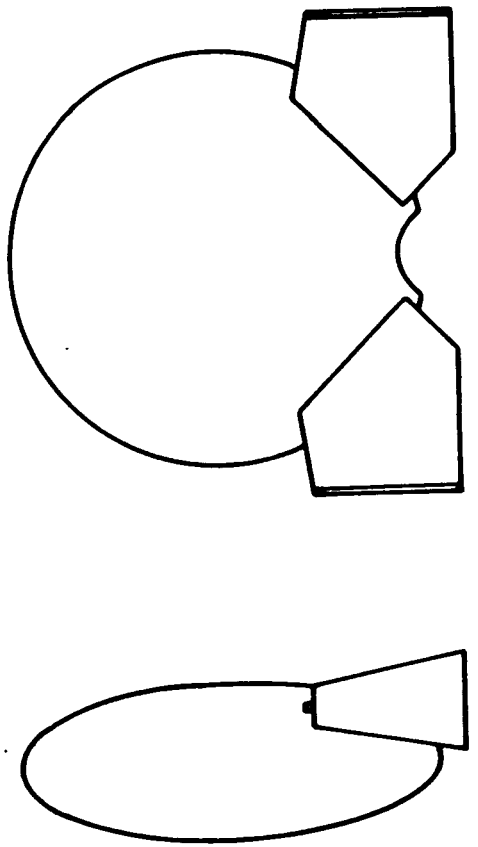

Figure 19.- Lenticular body.

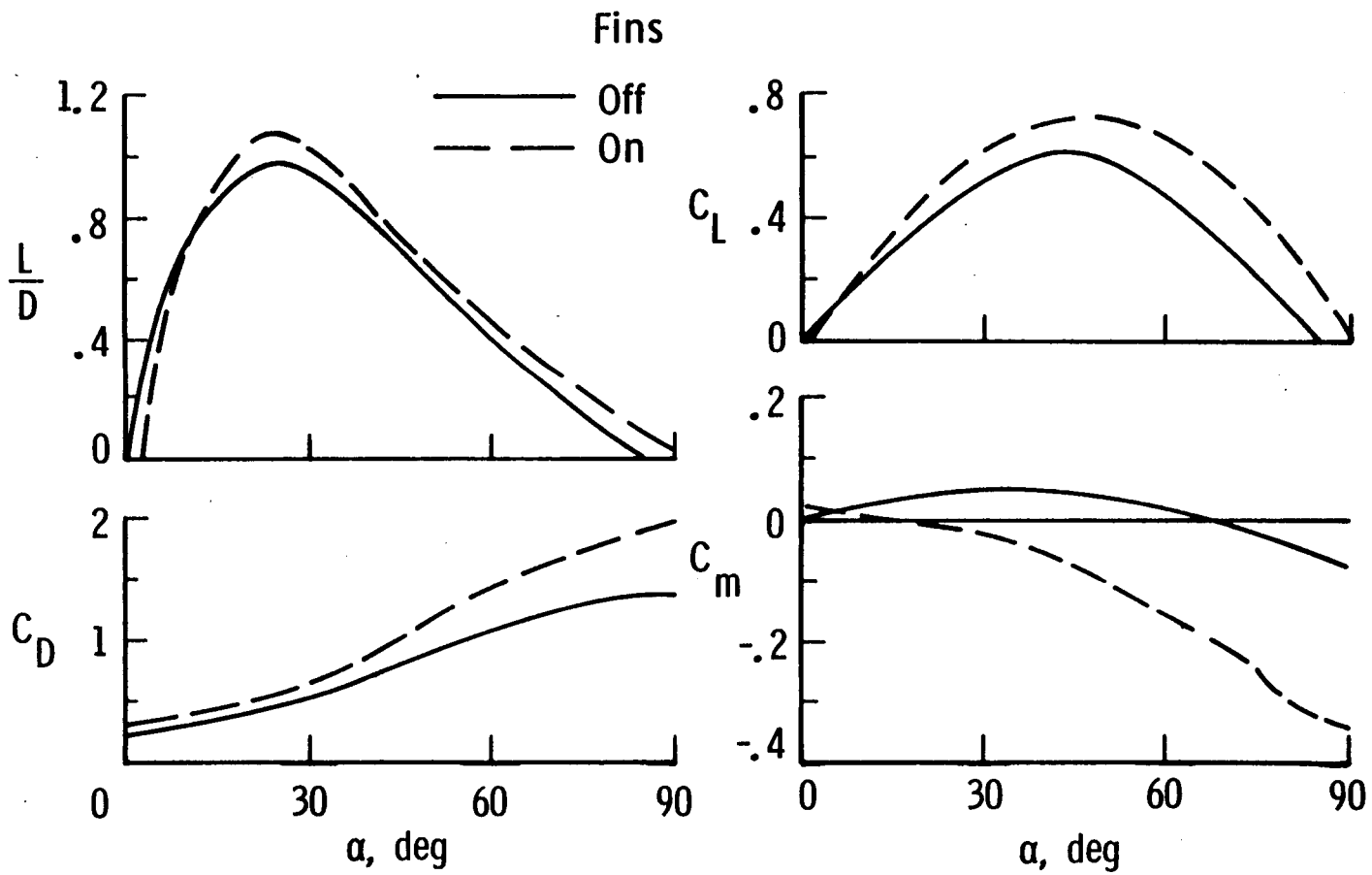

Figure 20.- Longitudinal characteristics, lenticular body, M = 2, c. g. = 0.45 ℓ.

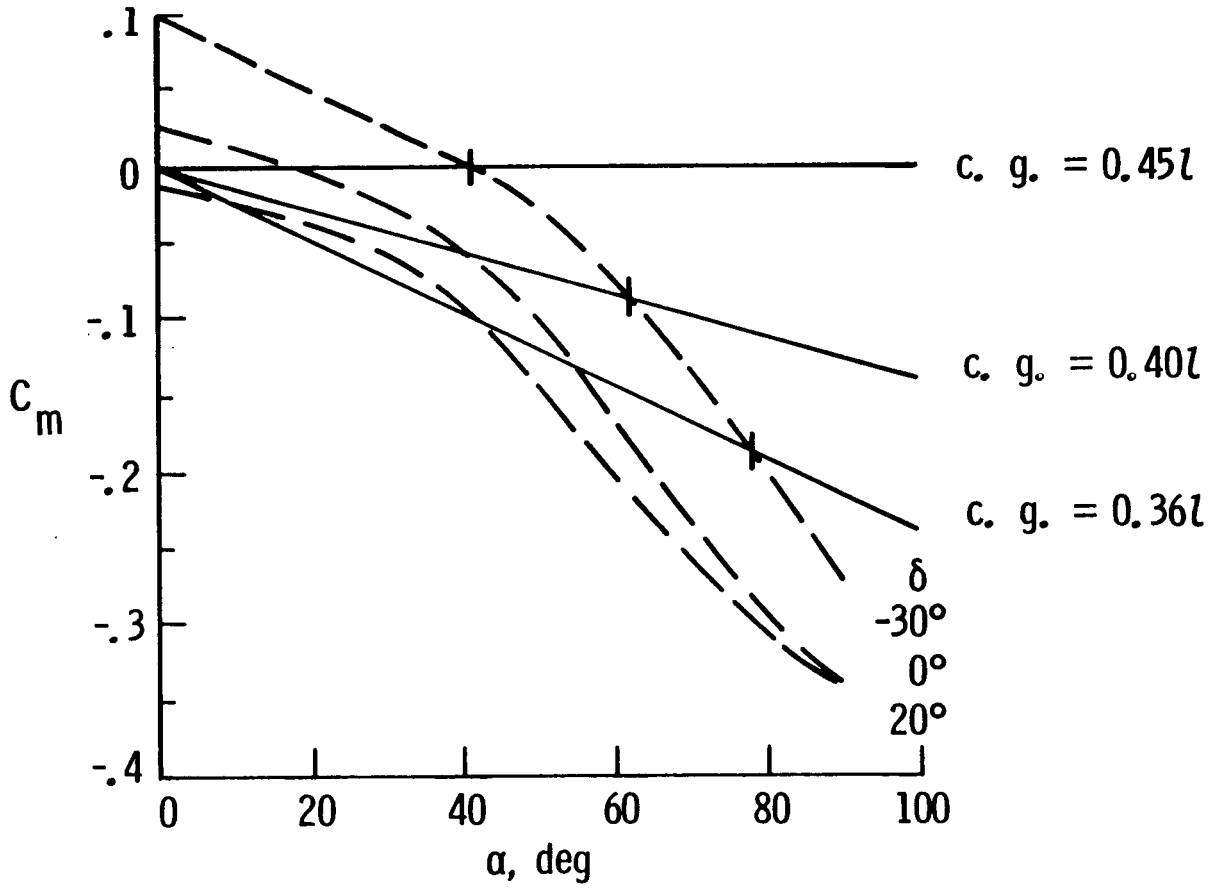

Figure 21.- Longitudinal control, lenticular body, M = 2.

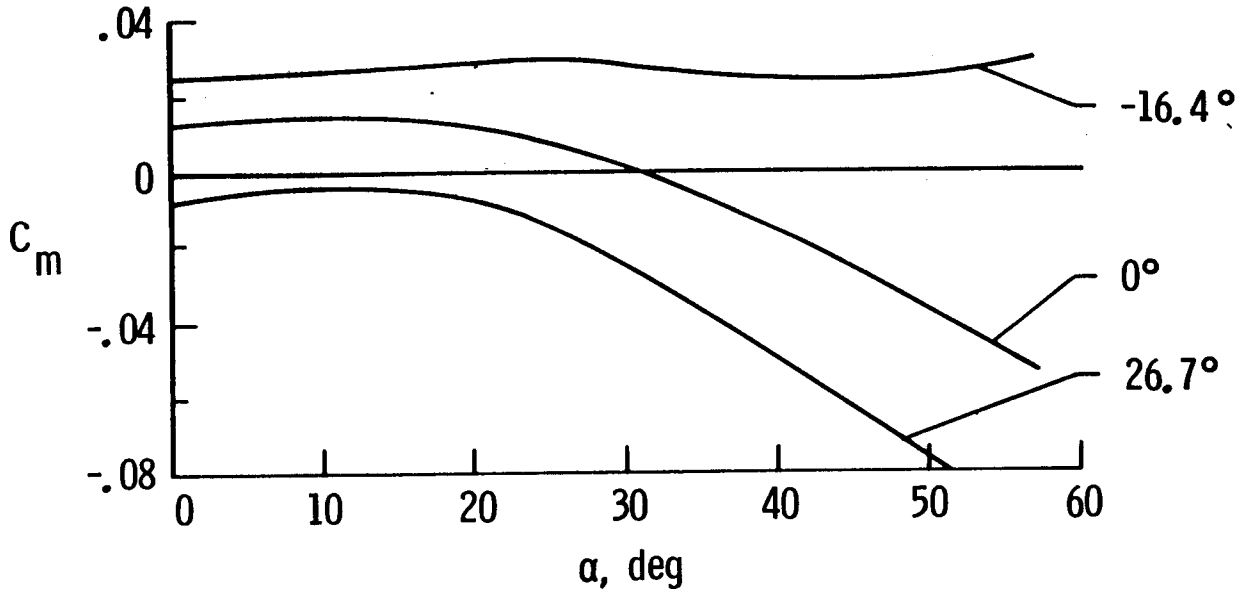

Figure 22.- Longitudinal control, lenticular body, M = 3.5, c.g. = 0.45 ℓ.

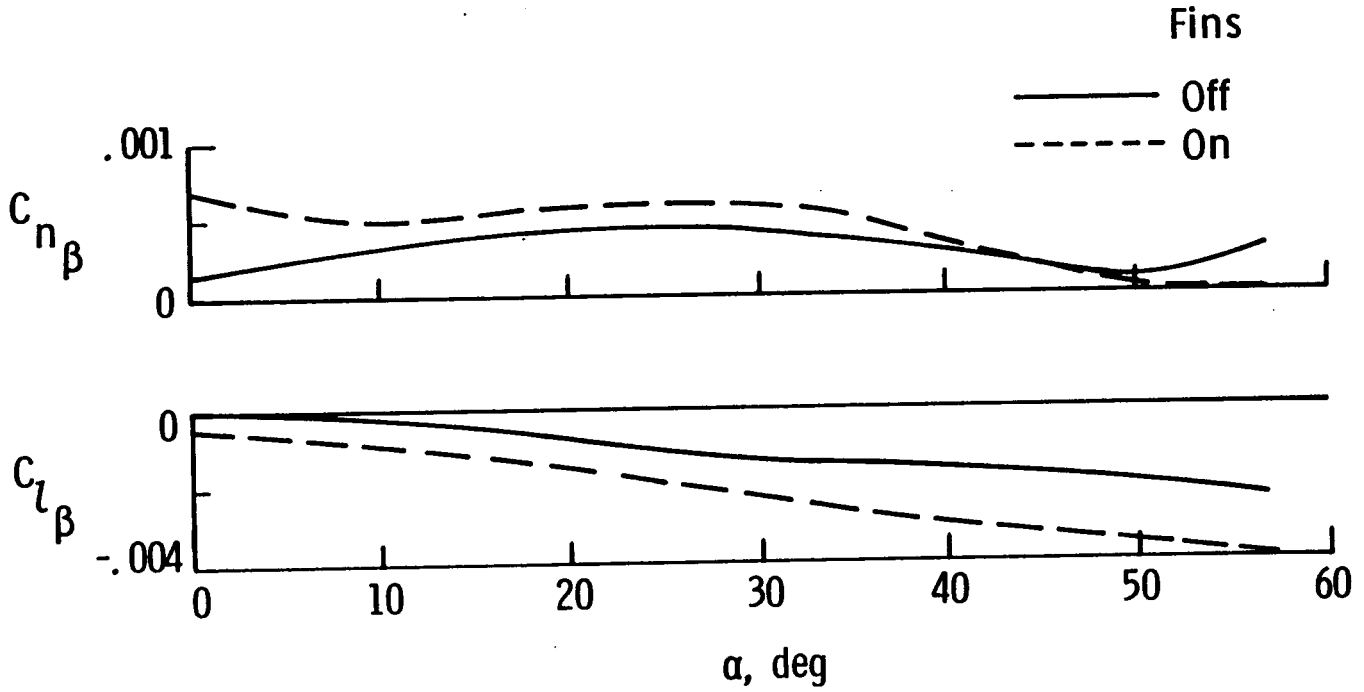

Figure 23.- Lateral-directional stability, lenticular body.
M = 3.5, c. g. = 0.45 ℓ.

1. Report No.	2. Government Accession No.	3. Recipient's Catalog No.
NASA TM-87645		

4. Title and Subtitle	5. Report Date
SUPERSONIC AERODYNAMIC CHARACTERISTICS OF SOME REENTRY CONCEPTS FOR ANGLES OF ATTACK TO 90°	November 1985
	6. Performing Organization Code 505-69-41-01

7. Author(s)	8. Performing Organization Report No.
M. Leroy Spearman	
	10. Work Unit No.
9. Performing Organization Name and Address NASA Langley Research Center Hampton, Virginia 23665-5225	11. Contract or Grant No.
	13. Type of Report and Period Covered
12. Sponsoring Agency Name and Address National Aeronautics and Space Administration Washington, DC 20546	14. Sponsoring Agency Code

15. Supplementary Notes

Colateral publication of AIAA Paper Number 85-1795-CP presented at the AIAA 12th Atmospheric Flight Mechanics Conference, Snowmass, Colorado, August 19-21, 1985.

16. Abstract

Past studies of reentry vehicles tested to high angles of attack (up to 90°) in the Mach number range from 2 to 4.8 are reviewed. Two basic planforms are considered--highly-swept deltas and circular. The delta concepts include variations in cross section (and thus volume) and in camber distribution. The effectiveness of various types of aerodynamic control devices is also included. The purpose of the paper is to examine the characteristics of the vehicles with a view toward the potential usefulness of such concepts in a flight regime that would include reentry from space into the atmosphere followed by a transition to sustained atmospheric flight.

17. Key Words (Suggested by Author(s))	18. Distribution Statement
Reentry vehicles High angle aerodynamics	Unclassified - Unlimited Subject Category 15

19. Security Classif. (of this report)	20. Security Classif. (of this page)	21. No. of Pages	22. Price
Unclassified	Unclassified	31	A03

For sale by the National Technical Information Service, Springfield, Virginia 22161